SUPPORTING INFORMATION

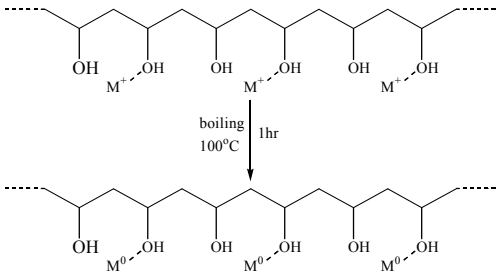

Figure S-1. Mechanism for the preparation of *M*-NPs in PVA (where *M* refers to Ag or Au).

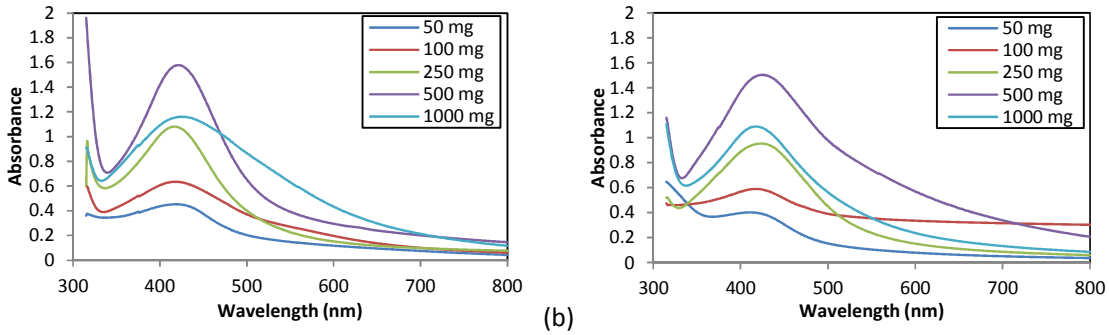

Figure S-2. UV-Vis absorption spectra of PVA (a) liquids and (b) films, containing AgNPs prepared from different loadings of $AgNO_3$ precursor.

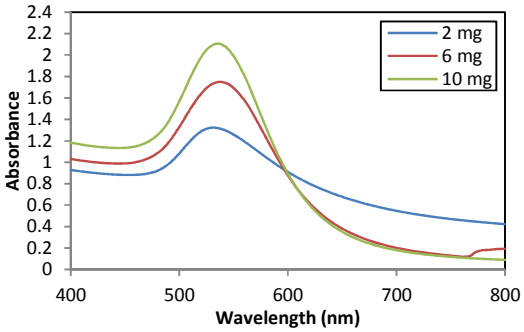

Figure S-3. UV-Vis absorption spectra of PVA liquids, containing AuNPs prepared from different loadings of $HAuCl_4$ precursor.

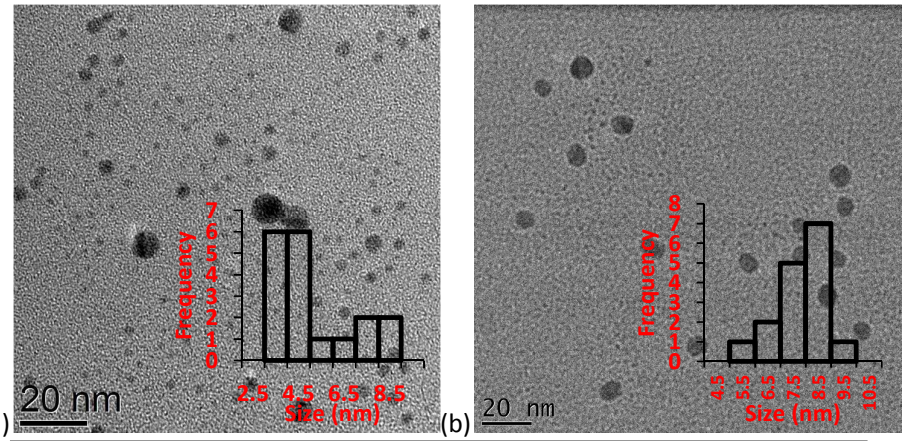

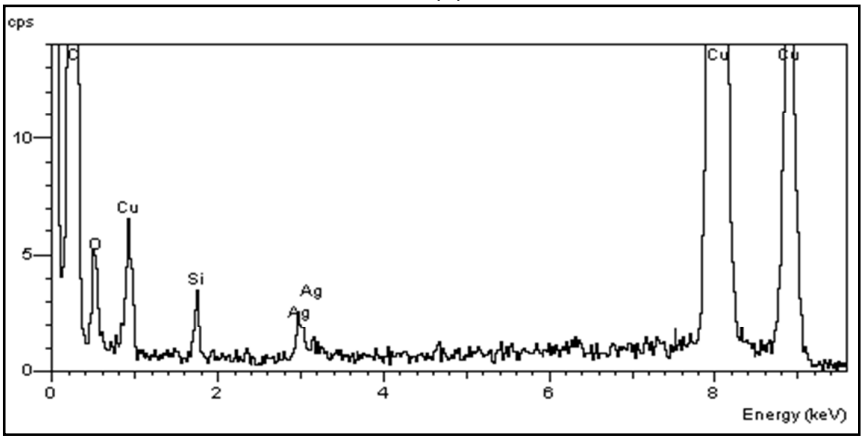

Figure S-4. TEM image of (a) PVA-AgNPs and (b) PVA-AgNPs-pphTEOS, with particle size distribution in the image area; (c) EDX spectrum of the PVA-AgNPs-pphTEOS film.

(a)

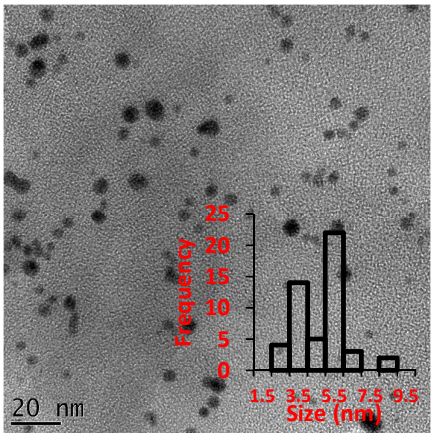

(b)

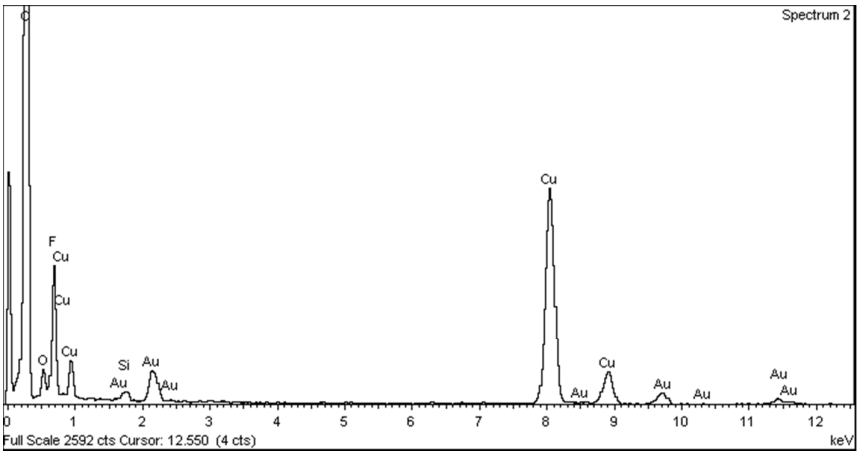

Figure S-5. TEM image of (a) PVA-AuNPs with particle size distribution in the image area; (b) EDX spectrum of the PVA-AuNPs-pphTEOS film.

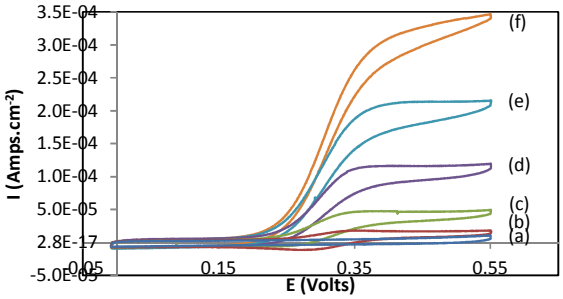

Figure S-6. Cyclic voltammograms of the PVA-pphTEOS-GOD graphite electrode in PBS (0.2 M, pH 7.0) (a) in the absence (b) and presence of FMCA (0.2 mM). Curves *c*, *d*, *e* and *f* are electrocatalytic responses to the oxidation of glucose in PBS (0.2 M, pH 7.0) containing 2.5 (c), 5.0 (d), 10.0 (e) and 20.0 mM (f) glucose, respectively, in the presence of FMCA (0.2 mM). Scan rate of 5 mV s^{-1}.

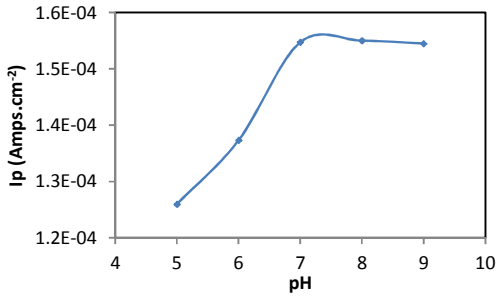

Figure S-7. The effect of buffer pH on current response of the PVA-pphTEOS-GOD electrode.

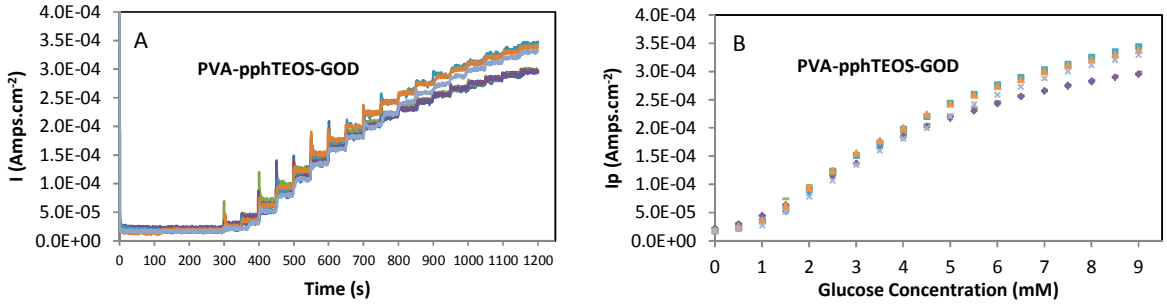

Figure S-8. *Current-time* curves obtained at the PVA-pphTEOS-GOD graphite electrodes for successive additions of 0.5 mM glucose. Conditions: 0.2 M pH 7.0 PBS in the presence of 0.8 mM FMCA; applied potential, 0.55 V (*vs.* Ag/AgCl). Plot B shows the calibration curves of the enzyme electrode as a function of glucose concentrations.

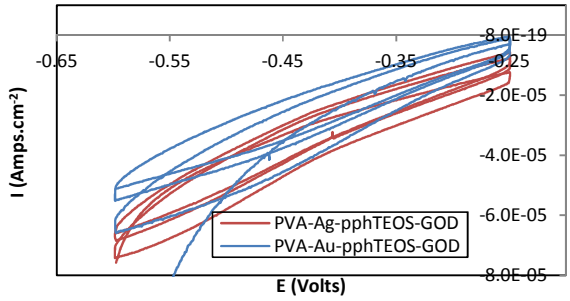

(a)

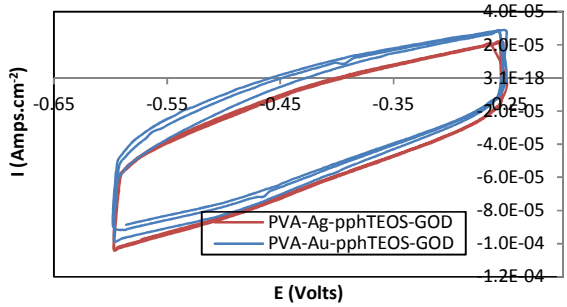

(b)

Figure S-9. Voltammograms of PVA-Ag/Au-pphTEOS-GOD graphite electrodes in pre-deaerated PBS (0.2 M, pH 7.0) at the scan rate (a) 5 mV s^{-1} and (b) 50 mV s^{-1}.

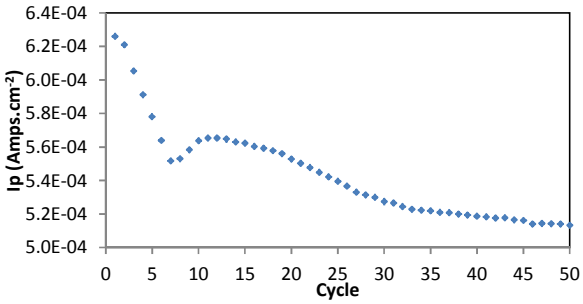

Figure S-10. Stability of the PVA-pphTEOS-GOD graphite electrode on continuous scanning.